

Inhibition of SARS-CoV-2 main protease by phenolic compounds from *Manilkara hexandra* (Roxb.) Dubard assisted by *in Silico* virtual screening

Fatma M. Abd El-Mordy¹, Mohamed M. El-Hamouly², Magda T. Ibrahim³, Gehad Abd El-Rheem⁴, Omar M. Aly⁵, Adel M. Abd El-kader^{6,7}, Khayrya A. Youssif⁸, Usama Ramadan Abdelmohsen^{6,9*}

¹Department of Pharmacognosy, Faculty of Pharmacy (Girls), Al-Azhar University, 11754 Cairo, Egypt.

²Department of Pharmacognosy, Faculty of Pharmacy (Boys), Al-Azhar University, 11371 Cairo, Egypt.

³Department of Pharmacognosy, Faculty of Pharmacy, Sinai University, 41636 Kantara Branch.

⁴Department of Pharmacology, National Research Centre, 12622 Giza, Egypt.

⁵Department of Medicinal Chemistry, Faculty of Pharmacy, Minia University, 61519 Minia, Egypt.

⁶Department of Pharmacognosy, Faculty of Pharmacy, Deraya University, 61111 Minia, Egypt

⁷Department of Pharmacognosy, Faculty of Pharmacy, Al-Azhar University, Assiut 71524, Egypt

⁸Department of Pharmacognosy, Faculty of Pharmacy, Modern University for Technology and Information, Cairo, Egypt.

⁹Department of Pharmacognosy, Faculty of Pharmacy, Minia University, 61519 Minia, Egypt.

***Corresponding author: Usama.ramadan@mu.edu.eg**

Table of Contents

Figure S1:	UV spectra of Compound I .	7
Figure S2:	¹ H-NMR spectrum of compound I in (DMSO- <i>d</i> ₆ -400 MHz).	8
Figure S3:	¹³ C-NMR spectrum of compound I in (DMSO- <i>d</i> ₆ -100 MHz).	9
Figure S4:	UV spectra of compound II .	10
Figure S5:	Negative ESI/MS spectra of compound II .	11
Figure S6:	¹ H-NMR spectrum of compound II in (DMSO- <i>d</i> ₆ -400 MHz).	12
Figure S7:	¹³ C-NMR spectrum of compound II in (DMSO- <i>d</i> ₆ -100 MHz).	13
Figure S8:	Partial expansion of the ¹³ C-NMR spectrum of compound II in (DMSO- <i>d</i> ₆ -100 MHz).	14
Figure S9:	¹ H-NMR spectrum of compound III in (DMSO- <i>d</i> ₆ -400 MHz).	15
Figure S10:	Partial expansion of the ¹ H-NMR spectrum of compound III in (DMSO- <i>d</i> ₆ -400 MHz).	16
Figure S11:	¹³ C-NMR spectrum of compound III in (DMSO- <i>d</i> ₆ -100 MHz).	17
Figure S12:	Partial expansion of the ¹³ C-NMR spectrum of compound III in (DMSO- <i>d</i> ₆ -100 MHz).	18
Figure S13:	DEPT-135 spectrum of compound III in (DMSO- <i>d</i> ₆ -100 MHz).	19
Figure S14:	¹ H-NMR spectrum of compound IV in (DMSO- <i>d</i> ₆ -400 MHz)	20
Figure S15:	Partial expansion of the ¹ H-NMR spectrum of compound IV in (DMSO- <i>d</i> ₆ -400 MHz).	21
Figure S16:	DEPT-135 spectrum of compound IV in (DMSO- <i>d</i> ₆ -100 MHz)	22
Figure S17:	Partial expansion of the DEPT-135 spectrum of compound IV in (DMSO- <i>d</i> ₆ -100 MHz).	23
Figure S18:	Metabolomic chromatogram of different extracts of <i>Manilkara hexandra</i> (Roxb.) Dubard.	24
Figure S19:	Metabolomic chromatogram of the ethyl acetate extract of <i>Manilkara hexandra</i> (Roxb.) Dubard bark.	25
Figure S20:	Metabolomic chromatogram of the methanol extract of <i>Manilkara hexandra</i> (Roxb.) Dubard leaves.	26

Methods:**Compound I**

UV/Vis λ_{max} (MeOH) *nm*: 254, 302, 377; (+ NaOMe): 284 sh, 317, 416; (+ NaOAc): 265, 332, 385; (+ NaOAc/H₃BO₃): 232.5, 258, 300; (+ AlCl₃): 269, 309 sh, 447 ;(+ AlCl₃/HCl): 269, 314, 428.

Positive MS, *m/z* 319 [M+H]⁺ for a MF: C₁₅H₁₀O₈.

¹H NMR (400 MHz, DEMSO-*d*₆, TMS as int. std , δ , ppm): 12.69 (br s, 1 H , 5-OH), 10.91-9.28 (br s , 4H, 7 , 3' , 4' , 5' - OH) 6.89 (s, 2H, H-2' , 6') , 6.39 (d, 1 H , *J*=2.1 Hz, H-8), 6.21 (d, 1 H , *J*=2.1 Hz, H - 6) , ¹³C NMR (100 MHz, DEMSO-*d*₆) 157.96 (C-2), 134.74 (C-3), 178.24 (C-4), 161.76 (C-5), 99.13 (C-6), 164.63 (C-7), 94.00 (C-8), 156.87 (C-9), 104.50 (C-10), 120.08 (C-1'), 108.38 (C-2' , C-6'), 146.22 (C-3' , C-5'), 136.91 (C-4').

Compound II

UV/Vis λ_{max} (MeOH) *nm*: 257.5, 301.5, 352.5; (+ NaOMe): 270.5 sh, 322, 391.5; (+ NaOAc): 271, 322.5, 381; (+ NaOAc/H₃BO₃): 265, 339, 376.5; (+ AlCl₃): 273, 312 sh, 365.5, 420 ;(+ AlCl₃/HCl): 272.5, 302.5, 369.5, 422.5.

Negative MS, *m/z* 463.0 [M-H]⁻ for a MF: C₂₁ H₁₉O₁₂, 316.04 [M- rhamnose]⁻.

¹H NMR (400 MHz, DEMSO-*d*₆, TMS as int. std , δ , ppm): 12.69 (br s, 1 H , 5-OH), 10.86-9.27 (br s , 4H, 7 , 3' , 4' , 5' - OH) , 6.90 (s, 2H, H-2' , 6') , 6.38 (d, 1 H , *J*=2 Hz, H-8), 6.21 (d, 1 H , *J*=2 Hz, H - 6) , 5.21 (br s, 1H, H-1" of rhamnose), 3.99-3.17 (m, sugar protons) , 0.86 (d, *J*= 6 Hz, 3H, rhamnose - CH₃), ¹³C NMR (100 MHz, DEMSO-*d*₆) 157.96 (C-2), 134.74 (C-3), 178.24 (C-4), 161.77 (C-5), 99.14 (C-6), 164.63 (C-7), 94.00 (C-8), 156.87 (C-9), 104.51 (C-10), 120.09 (C-1') , 108.38 (C-2' , C-6') , 146.22 (C-3' , C-5') , 136.91 (C-4') , 102.37 (C-1'') , 70.85 (C-2'') , 71.02 (C-3'') , 71.73 (C-4'') , 70.48 (C-5'') , 17.99 (C-6'') .

Compound III

UV/Vis λ_{max} (MeOH) *nm*: 265, 298sh, 338sh; (+ NaOMe): 271, 328sh, 372; (+ NaOAc): 272, 340sh; (+ NaOAc/H₃BO₃): 265, 305, 340sh; (+ AlCl₃): 274, 302, 340, 392sh; (+ AlCl₃/HCl): 274, 302, 340, 392sh.

Positive MS, *m/z* 479.0 [M + H]⁺ for a MF: C₂₂H₂₂O₁₂, 333 [aglycon + H]⁺.

¹H NMR (400 MHz, DEMSO-*d*₆, TMS as int. std , δ , ppm) 12.58 (br s, 1 H , 5-OH), 10.95-9.47 (br s , 3H, 7 , 3' , 5' - OH) 6.82 (s, 2H, H-2' , 6') , 6.39 (d, 1 H , *J*=2.1 Hz, H-8), 6.22 (d, 1 H , *J*=2.1 Hz, H - 6) , 5.16 (br s, 1H, H-1" of rhamnose), 3.75 (s , 3H, 4'-OCH₃), 3.99-3.15 (m, sugar protons) , 0.83 (d, *J*=6 Hz, 3H, rhamnose - CH₃),

¹³C NMR (100 MHz, DEMSO-*d*₆) 157.91 (C-2), 135.17 (C-3), 178.04 (C-4), 161.36 (C-5), 99.30 (C-6), 164.44 (C-7), 94.33 (C-8), 156.94 (C-9), 104.67 (C-10), 125.034 (C-1'), 108.83 (C-2', C-6'), 150.73 (C-3', C-5'), 138.20 (C-4'), 102.28 (C-1''), 70.33 (C-2''), 70.96 (C-3''), 71.40 (C-4''), 70.52 (C-5''), 17.42 (C-6''), 60.45 (C4'-O-CH₃).

Compound IV

Positive MS, m/z, 641 [M + H]⁺ for a MF: C₂₈H₃₂O₁₇.

¹H NMR (400 MHz, DEMSO-*d*₆, TMS as int. std, δ, ppm): 12.58 (br s, 1H, 5-OH), 10.89-9.47 (br s, 3H, 7, 3', 5' - OH) 6.82 (s, 2H, H-2', 6'), 6.38 (d, 1H, *J*=2 Hz, H-8), 6.22 (d, 1H, *J*=2 Hz, H-6), 5.16 (br s, 1H, H-1''' of rhamnose), 4.95 (d, 1H, *J*=6.6 Hz, H-1'' of glucose), 3.75 (s, 3H, 4'-OCH₃), 4.15-3.15 (m, sugar protons), 0.82 (d, *J*=5.8 Hz, 3H, rhamnose - CH₃). ¹³C NMR (100 MHz, DEMSO-*d*₆) (**Table 2**) 157.91 (C-2), 135.17 (C-3), 178.04 (C-4), 161.36 (C-5), 99.25 (C-6), 164.44 (C-7), 94.12 (C-8), 156.94 (C-9), 104.67 (C-10), 129.12 (C-1'), 109.09 (C-2', C-6'), 150.73 (C-3', C-5'), 138.20 (C-4'), 102.63 (C-1''), 73.64 (C-2''), 77.13 (C-3''), 70.51 (C-4''), 77.50 (C-5''), 67.87 (C-6''), 101.23 (C-1'''), 70.80 (C-2'''), 71.01 (C-3'''), 71.62 (C-4'''), 69.87 (C-5'''), 17.93 (C-6'''), 60.24 (C4'-O-CH₃).

Results and discussion:

Compound I was obtained as a yellow amorphous powder (35mg), melting point 357-359 °C. It exhibited a yellow fluorescence spot under long UV light turned to yellowish orange with Naturstoff and gave a faint blue color with FeCl₃. UV spectrum of compound I (Supplementary Materials, Figure S1) indicates a flavonol nucleus with free OH at 4' position, the free hydroxyl group at C-3, C-5, C-7, and orthodihydroxy group at 3' and 4' position. The ¹H-NMR spectrum (Supplementary Materials, Figure S2) exhibited a characteristic meta-coupled proton signal at δ 6.21 (1H, d, *J* = 1.4 Hz) and 6.38 (1H, d, *J* = 1.4 Hz) corresponding to H-6 and H-8 of flavonoid A ring. The other AX coupling system at δ 6.89 (2H, br s) was assigned to H-2' and H-6' of B ring. The ¹³C-NMR spectrum of **I** (Supplementary Materials, Figure S3) revealed the presence of 15 carbon signals from which two signals were representing two equivalent carbons δ 146.03 at (C-3', 5') and δ 108.38 (C-2', 6') pairs of equivalent carbons. Eight carbon resonances are aromatic oxygenated at δ 164.63 (C-7), 161.76 (C-5), 156.87 (C-9), 157.96 (C-2), 134.79 (C-4'), 134.74 (C-3), six aromatic non-oxygenated carbons at δ 120.08 (C-1'), 108.38 (C-2'/6'), 104.50 (C-

10), 99.13 (C-6), 94.00 (C-8) and one carbonyl signal at 178.24(C-4). By comparing the NMR spectral data with those reported in the literature, the structure of compound **I** was determined as 3, 5, 7, 3', 4', 5'- hexahydroxy – flavone (Myricetin)²⁹.

Compound II was obtained as a yellow amorphous powder (578 mg). A deep purple fluorescence spot appeared under long UV light turned to yellowish-orange color with Naturstoff and faint blue color with FeCl₃. UV spectrum of compound **II** (Supplementary Materials, Figure S4) is similar to that of compound **I**. Its molecular formula was established as C₂₁H₂₀O₁₂ based on an ion peak [M-H]⁻ at m/z 463 in -ve ESI/MS (Supplementary Materials, Figure S5). The spectroscopic data of **II** were similar to **I** (Supplementary Materials, Figure S6, S7, S8) except for the appearance of an α -L-rhamnopyranosyl moiety. So, the ¹H-NMR spectrum of **II** (Supplementary Materials, Figure S6) showed the presence of an anomeric proton signal at δ 5.21 (1H, br s), a methyl signal at δ 0.86 (3H, d, J = 6 Hz) and of six additional carbon signals at δ 102.37 (C-1"), 70.85 (C-2"), 71.02 (C3"), 71.73 (C-4"), 70.48 (C-5"), and 17.99 (C-6"). From these data together with ¹³C-NMR spectral data (Supplementary Materials, Figure S7, S8) indicating compound **II** was identified as Myricetin 3-*O*- α -L-C₄ rhamnopyranoside (Myricitrin)³⁰

Compound III was obtained as yellow needles (19 mg), on PC. It showed a purple spot under UV and UV/NH₃. Its spectroscopic data were similar to compound **II** (Supplementary Materials, Figure S9-S13). The ¹H-NMR spectrum of **III** showed myricetin skeleton in addition to the presence of an anomeric proton signal of rhamnose at δ 5.16 (1H, br s), a methyl signal at δ 0.83 (3H, d, J = 6 Hz) and an additional singlet signal at δ 3.75 (s, 3H) indicating 4'-OCH₃ (Supplementary Materials, Figure S9, S10). ¹³C-NMR spectrum of compound **III** showed carbon resonances which are characteristic for myricetin aglycone in addition to six carbon signals of rhamnose moiety at δ 102.28 (C-1"), 70.33 (C-2"), 70.96 (C3"), 71.40 (C-4"), 70.52 (C-5"), and 17.42 (C-6") and an additional signal at δ 60.45 indicating 4'-OCH₃ (Supplementary Materials, Figure S11, S12, S13). From the previous data, compound **III** was identified as Myricetin-4'-*O*-methyl ether-3-*O*- α -L-rhamnopyranoside (**Mearnsitrin**)¹⁹.

Compound IV was obtained as a dark yellow amorphous powder (16.6 mg), on PC. it showed a purple spot under UV and UV/NH₃. *UV/Vis* λ_{max} data is similar to that of compound **III**. Compound **IV** gives the typical signals of myricetin aglycon in ¹H-

NMR and ^{13}C -NMR (Supplementary Materials, Figure S14-S17), in addition to a single signal in ^1H -NMR at 3.75 representing 3H indicating the presence of methoxy group, the OCH₃ position is confirmed by ^{13}C -NMR which shows a downfield shift of C-4' to δ 138.20 and a signal at δ 60.24 ppm indicating C-4'-OCH₃ (similar to compound **III**). In addition to the presence of the two anomeric protons in the ^1H -NMR spectrum (Supplementary Materials, Figure S14-S15) at δ 5.16 (1H, br s) and δ 4.95 (**1H,d**, J= 6.6 Hz) together with a signal at 0.82 (**d**, J=5.8 Hz), and two anomeric carbons in the ^{13}C -NMR spectrum (Supplementary Materials, Figure S16-S17) at δ 101.23 and δ 102.63 ppm indicating rhamnose and glucose sugar moiety respectively, the downfield shift of C-6" of glucose to δ 67.87 indicating rutinose structure. From these data, compound IV was identified as Mearnsetin-3-O- β -D-rutinoside ¹⁹.

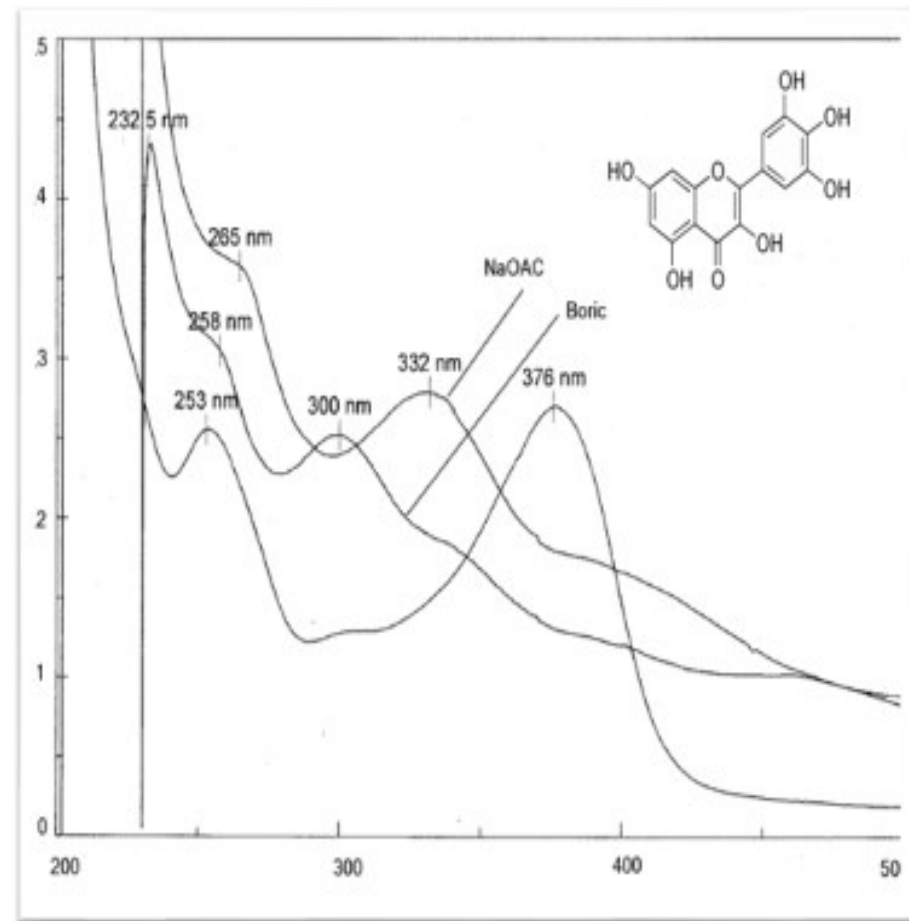
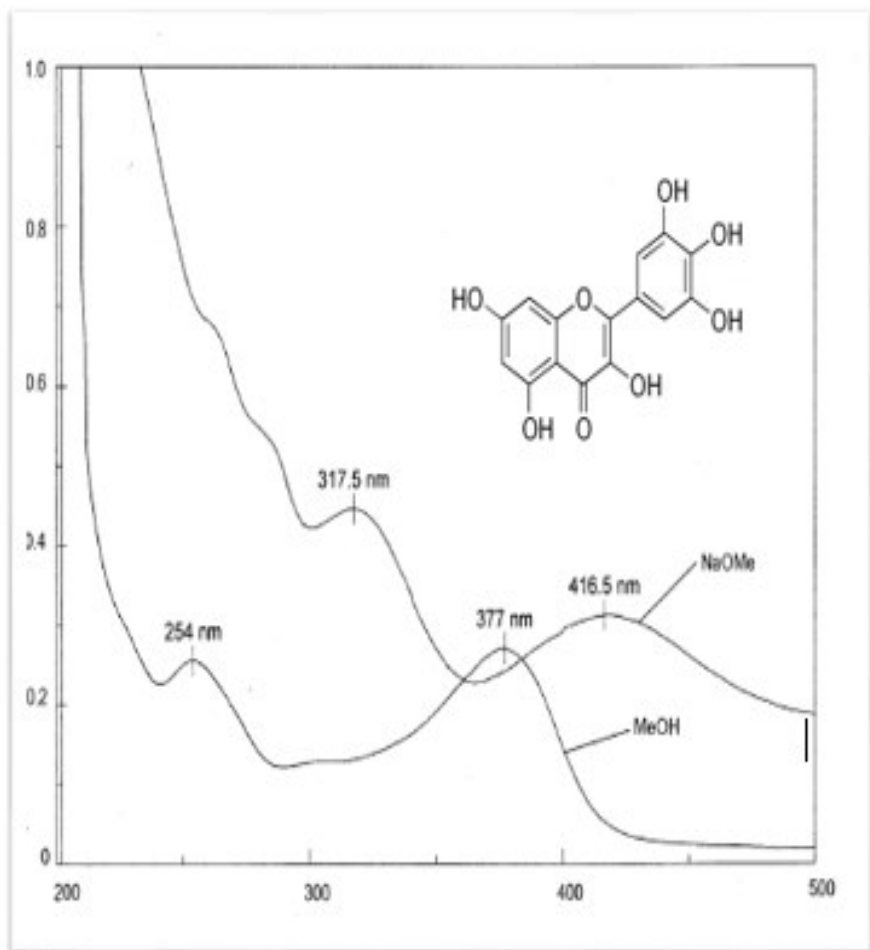


Figure S1: UV spectra of Compound I

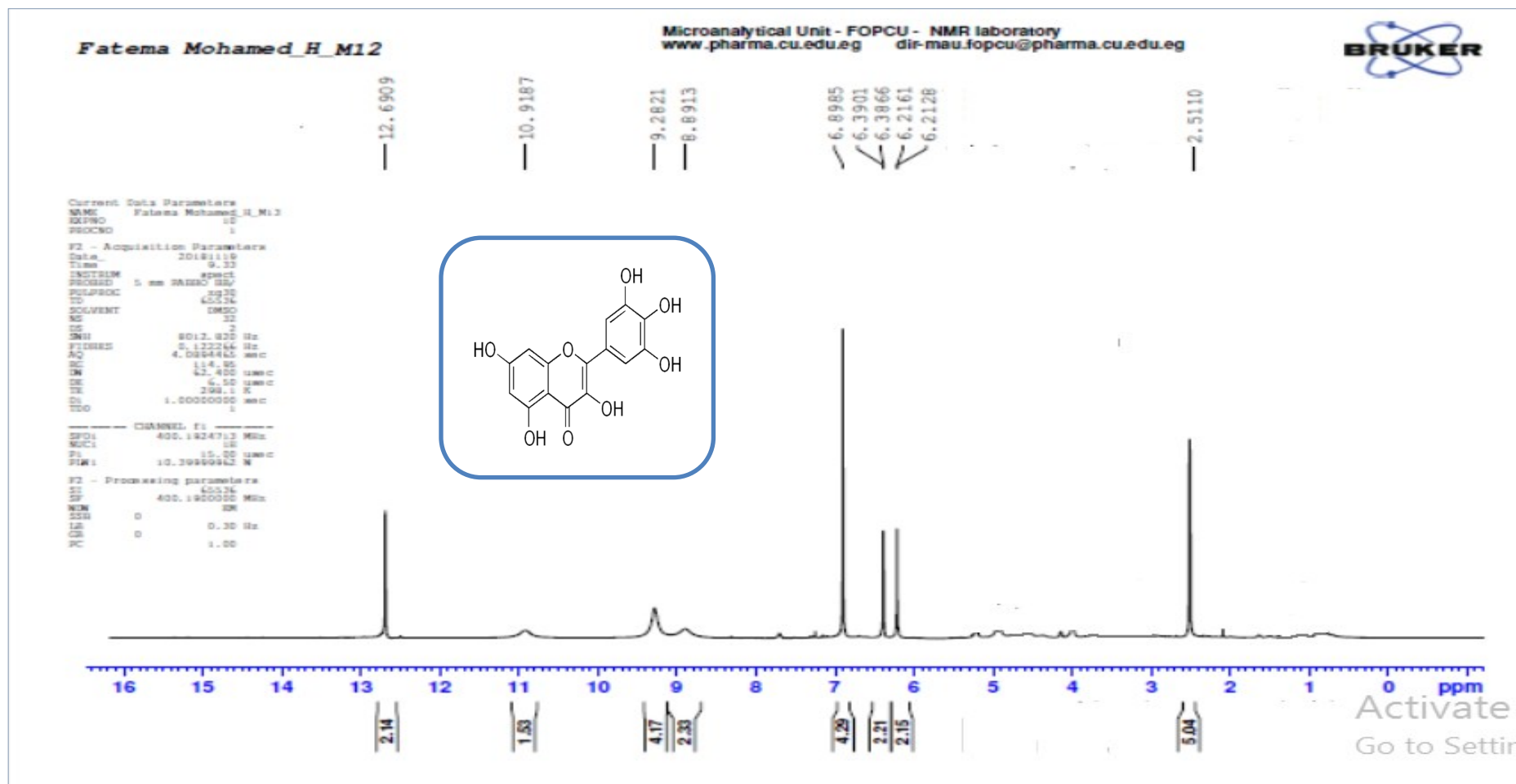


Figure S2: ¹H-NMR spectrum of compound I in (DMSO-*d*₆-400 MHz)

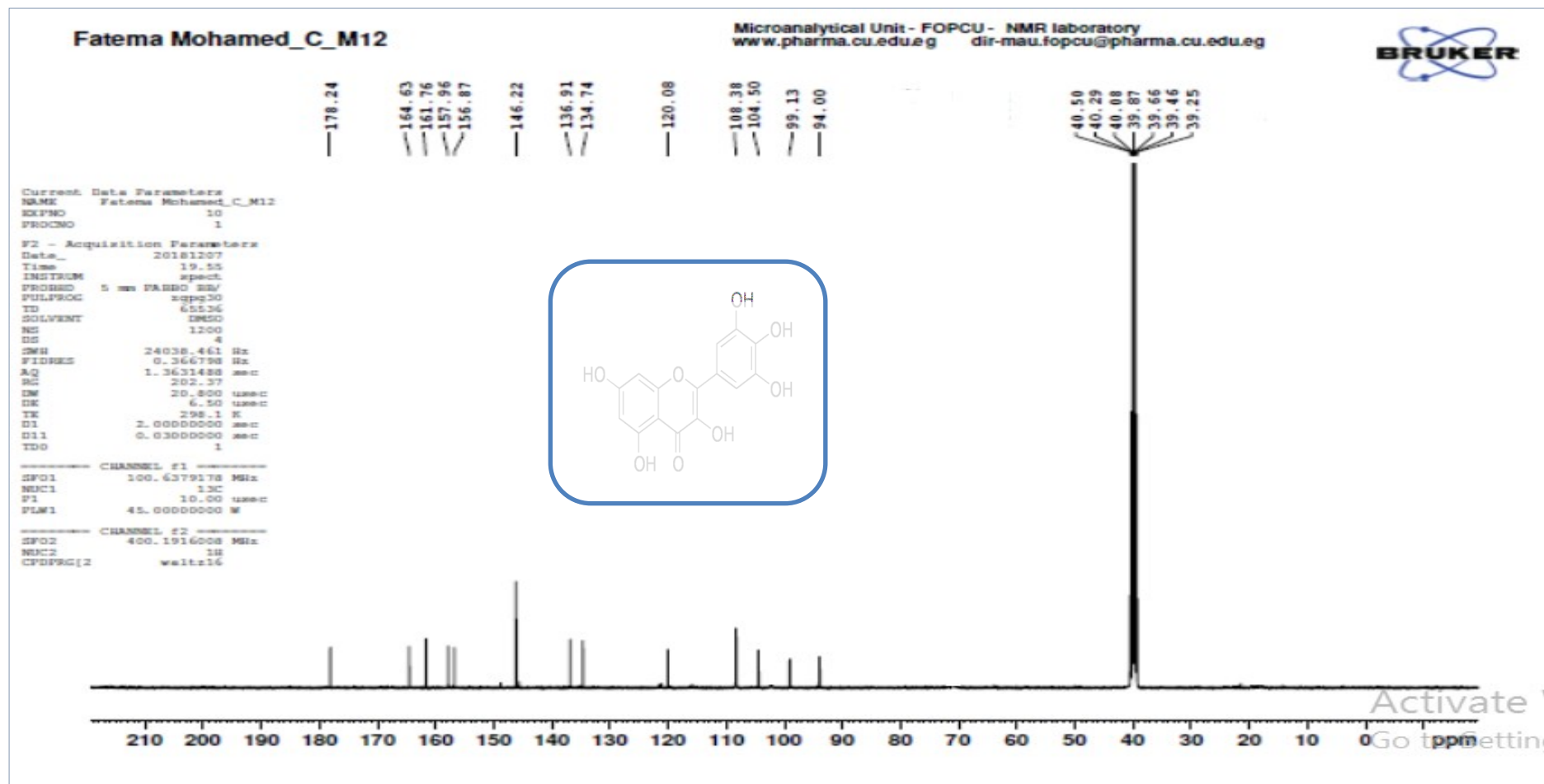


Figure S3: ¹³C-NMR spectrum of compound I in (DMSO-*d*₆-100 MHz)

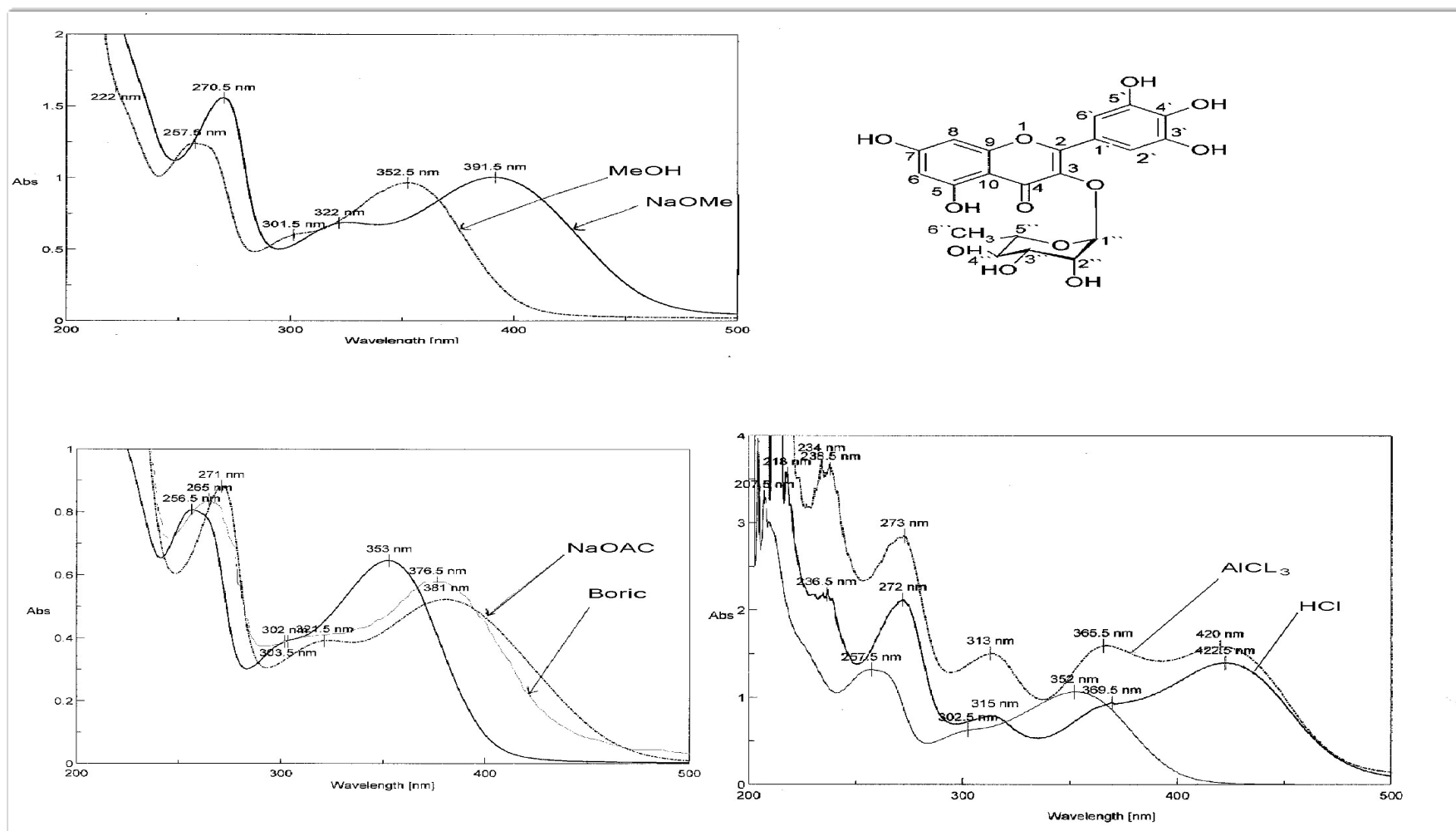


Figure S4: UV spectra of Compound II

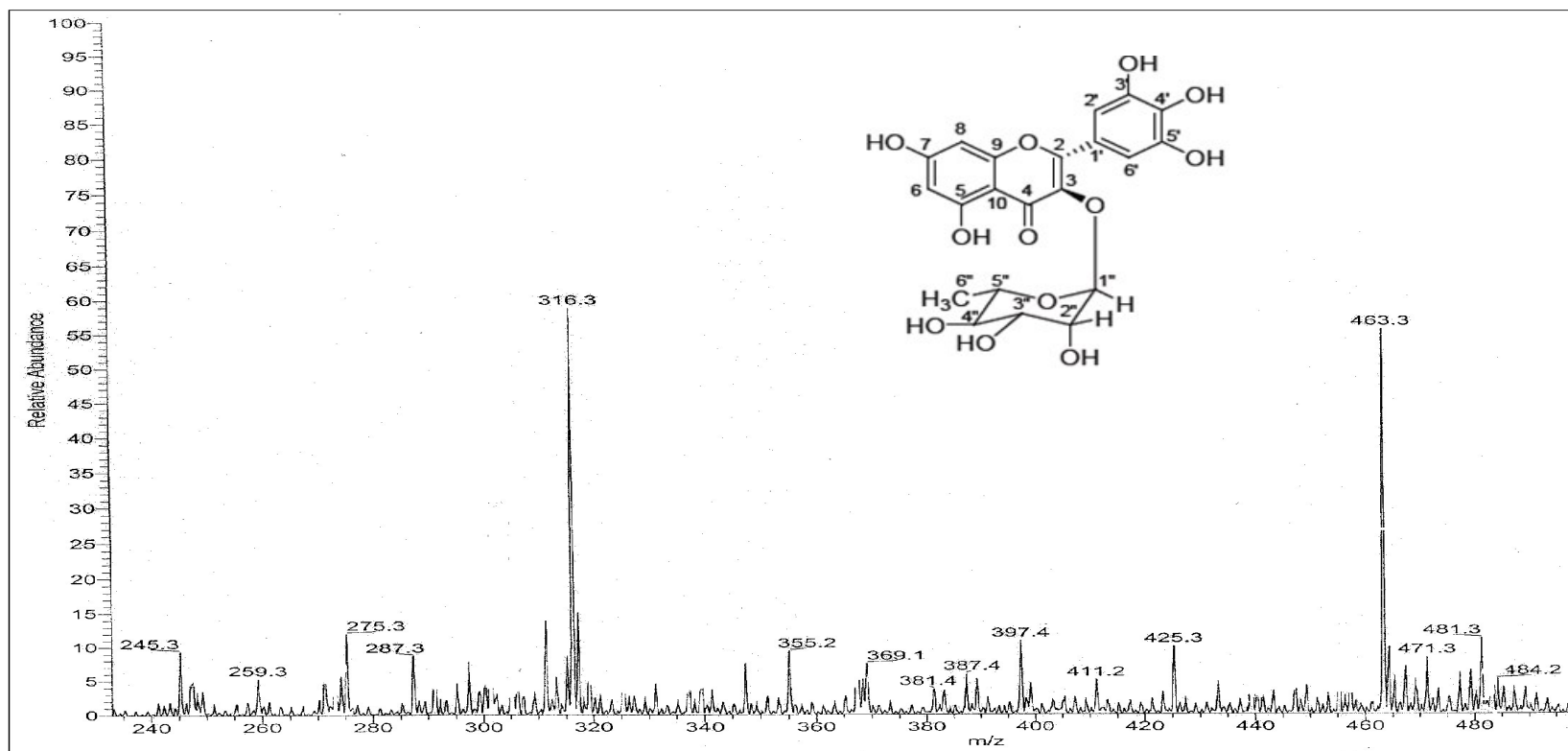


Figure S5: Negative ESI/MS spectra of compound II.

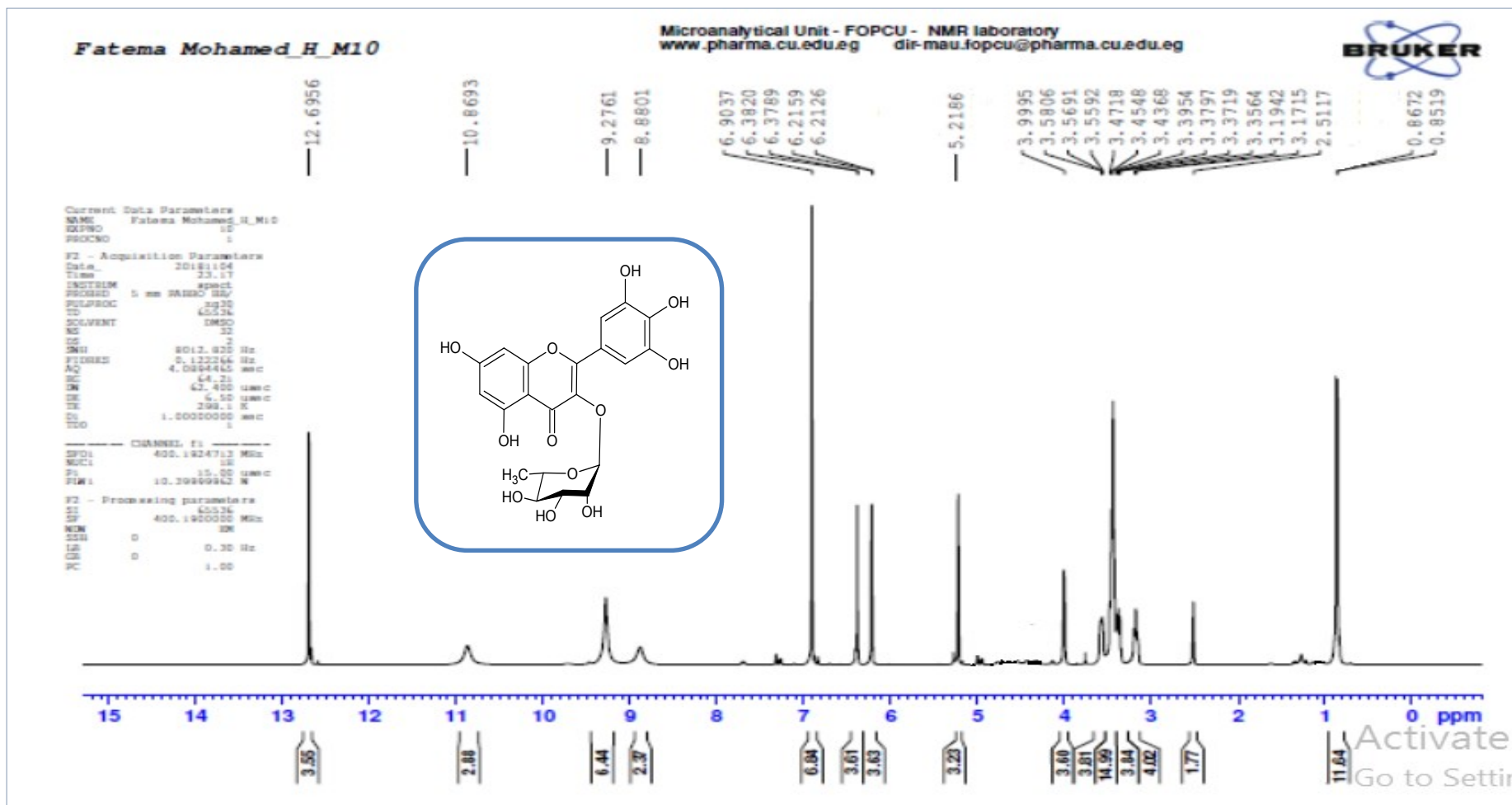
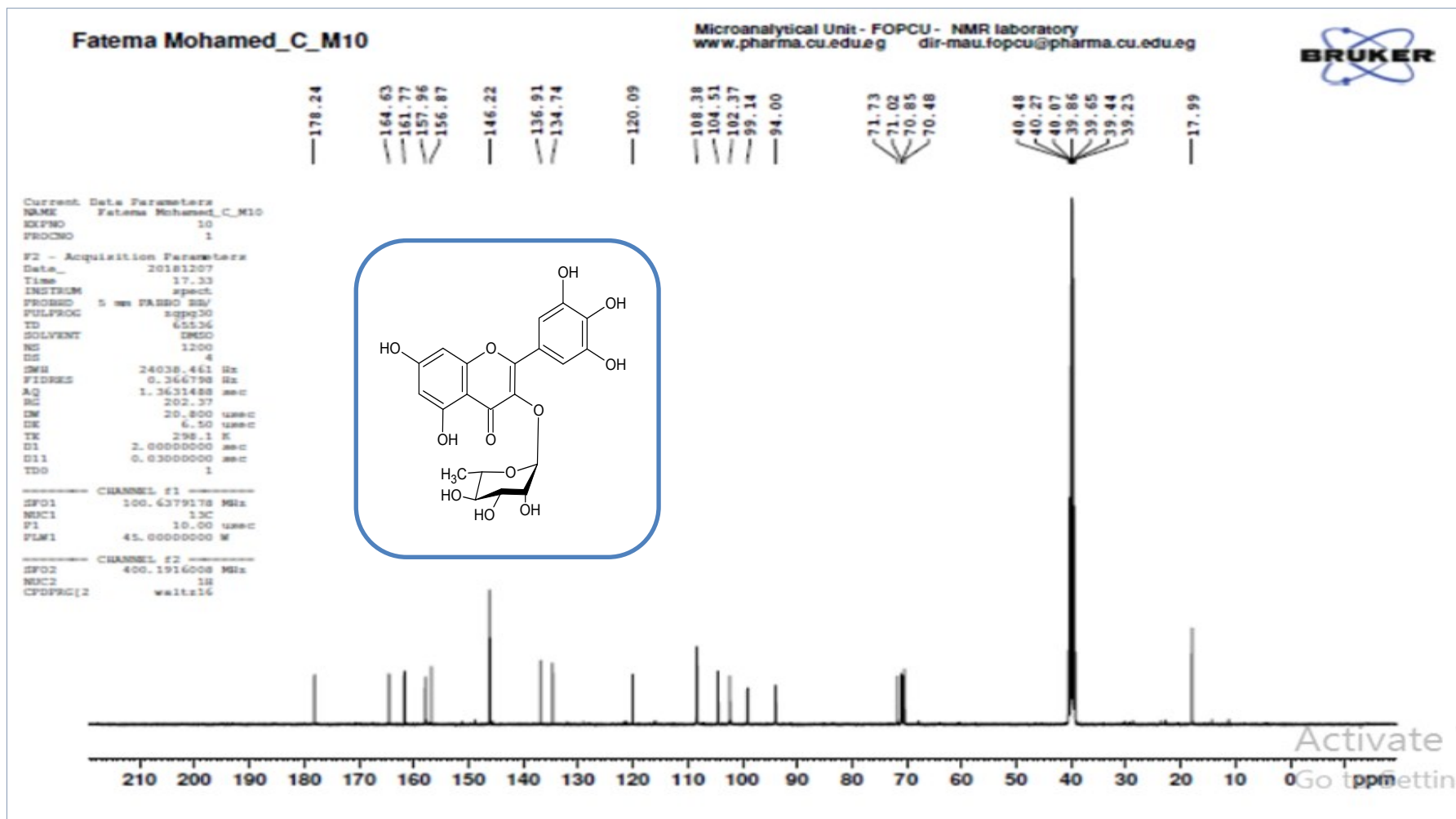


Figure S6: ¹H-NMR spectrum of compound II in (DMSO-d₆, 400 MHz)



Figur

e S7: ^{13}C -NMR spectrum of compound II in (DMSO- d_6 , 100 MHz)

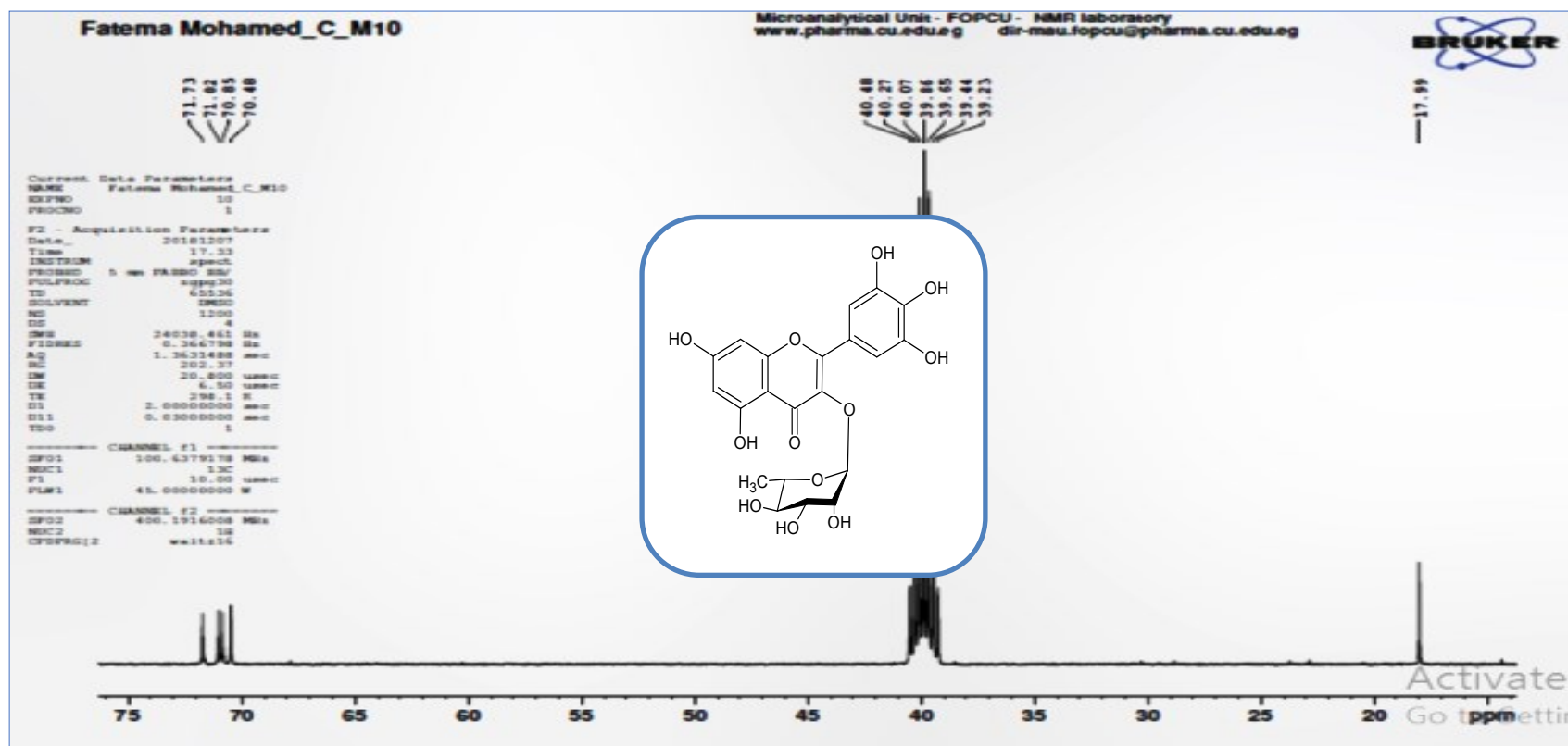


Figure S8: Partial expansion of the ^{13}C -NMR spectrum of compound **II** in ($\text{DMSO-}d_6$, 100 MHz)

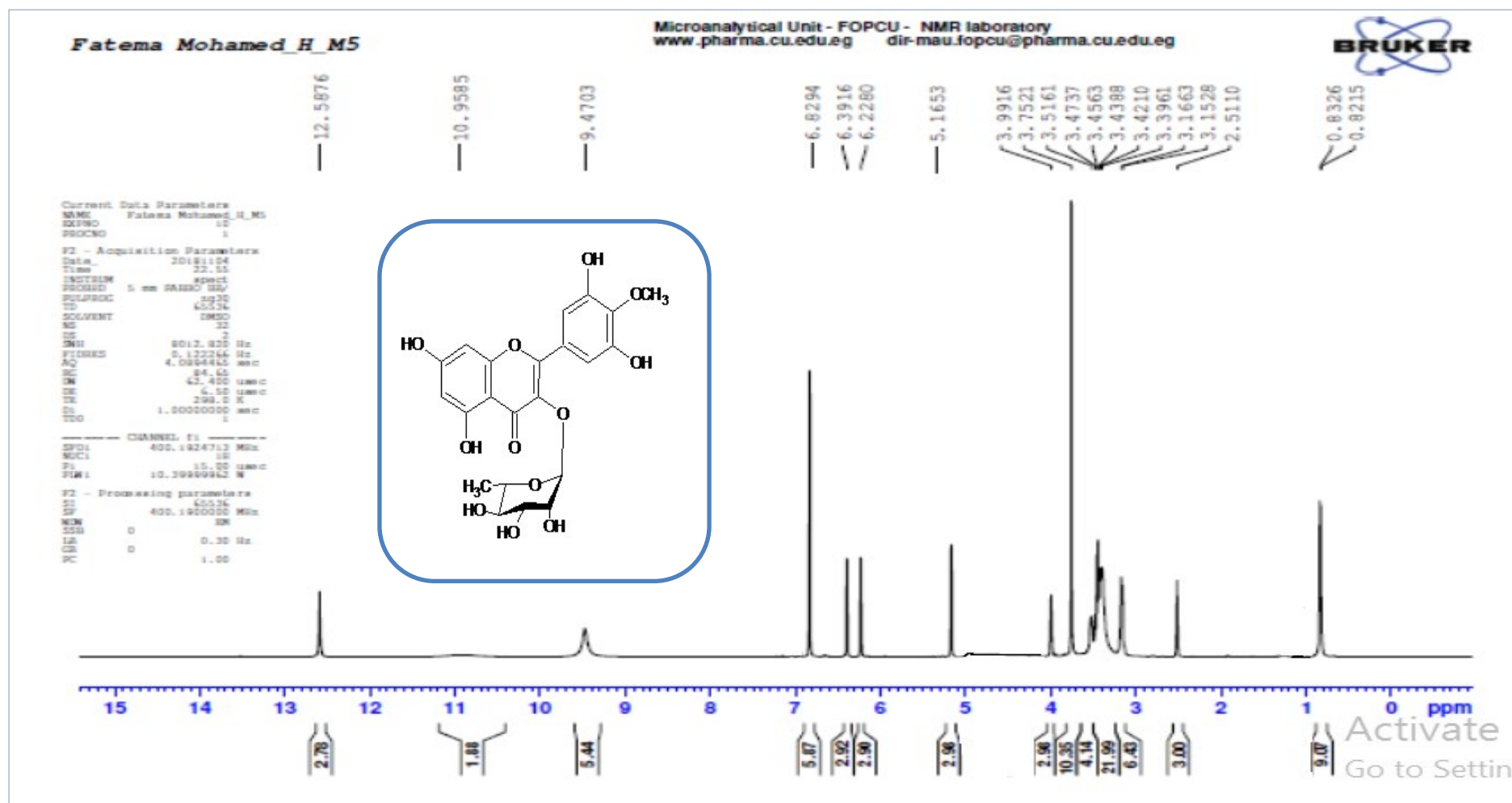


Figure S9: ¹H-NMR spectrum of compound **III** in (DMSO-*d*₆, 400 MHz)

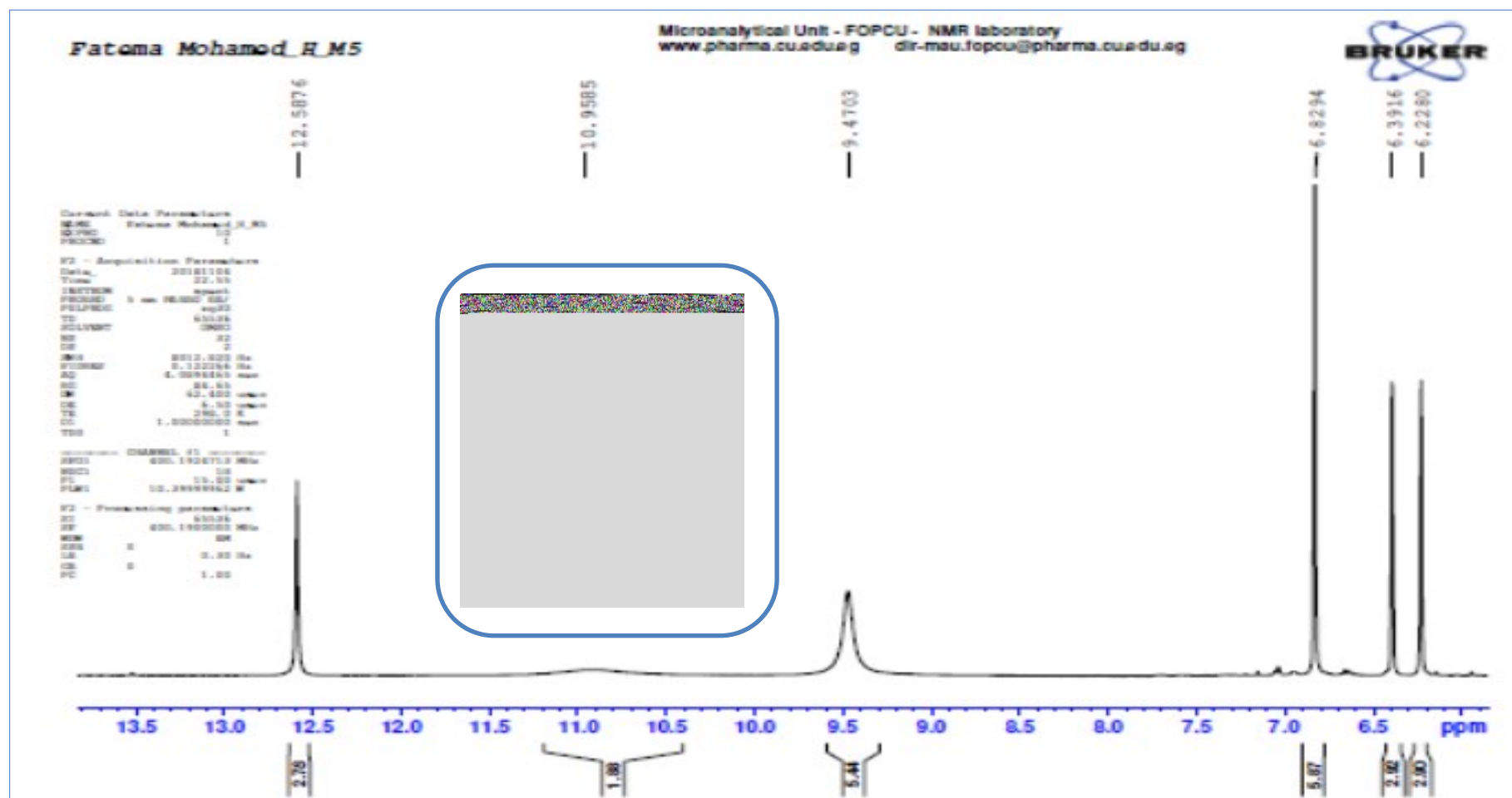


Figure S10: Partial expansion of the ^1H -NMR spectrum of compound **III** in ($\text{DMSO-}d_6$, 400 MHz)

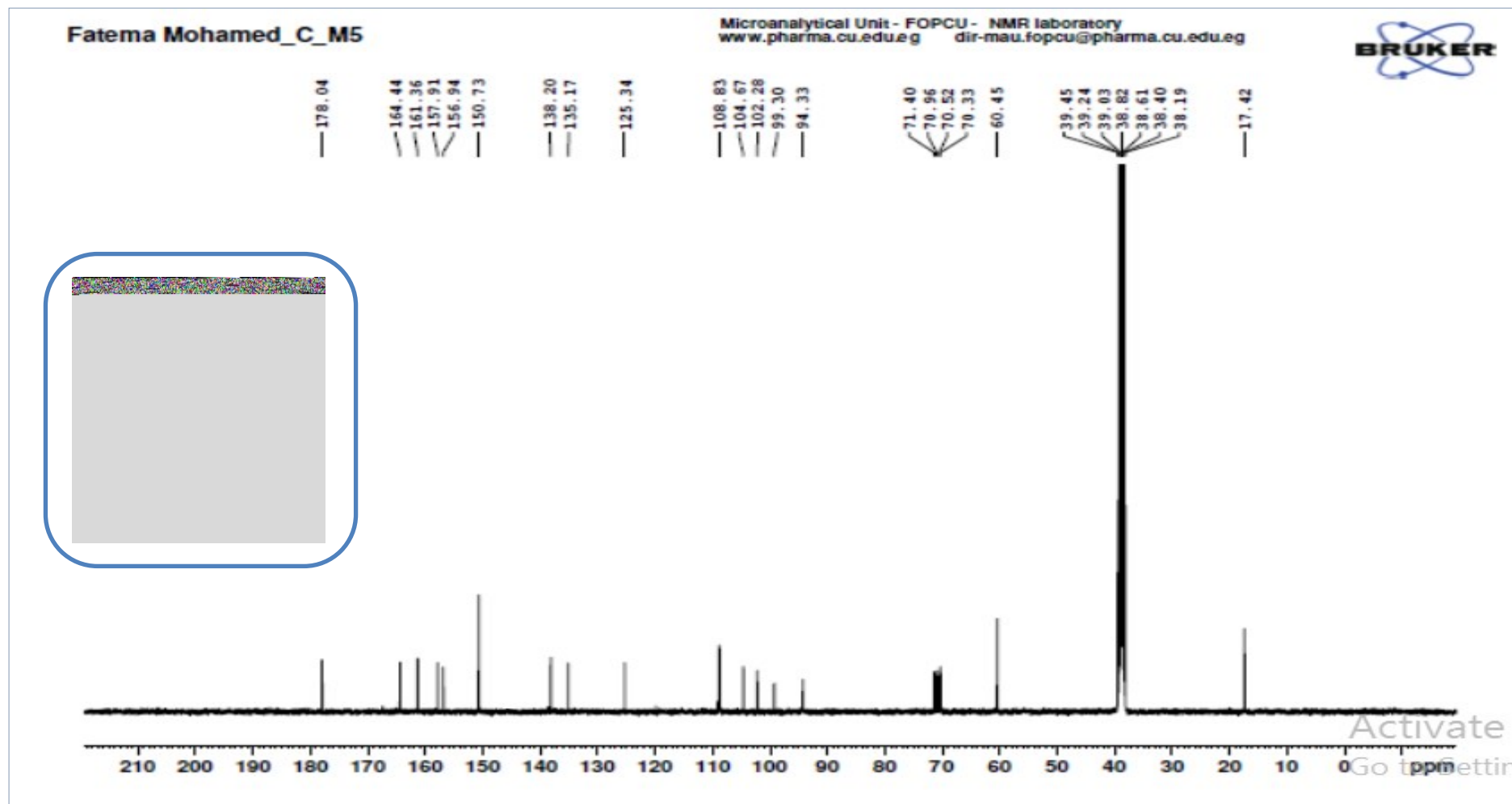


Figure S11: ^{13}C -NMR spectrum of compound **III** in ($\text{DMSO-}d_6$, 100 MHz)

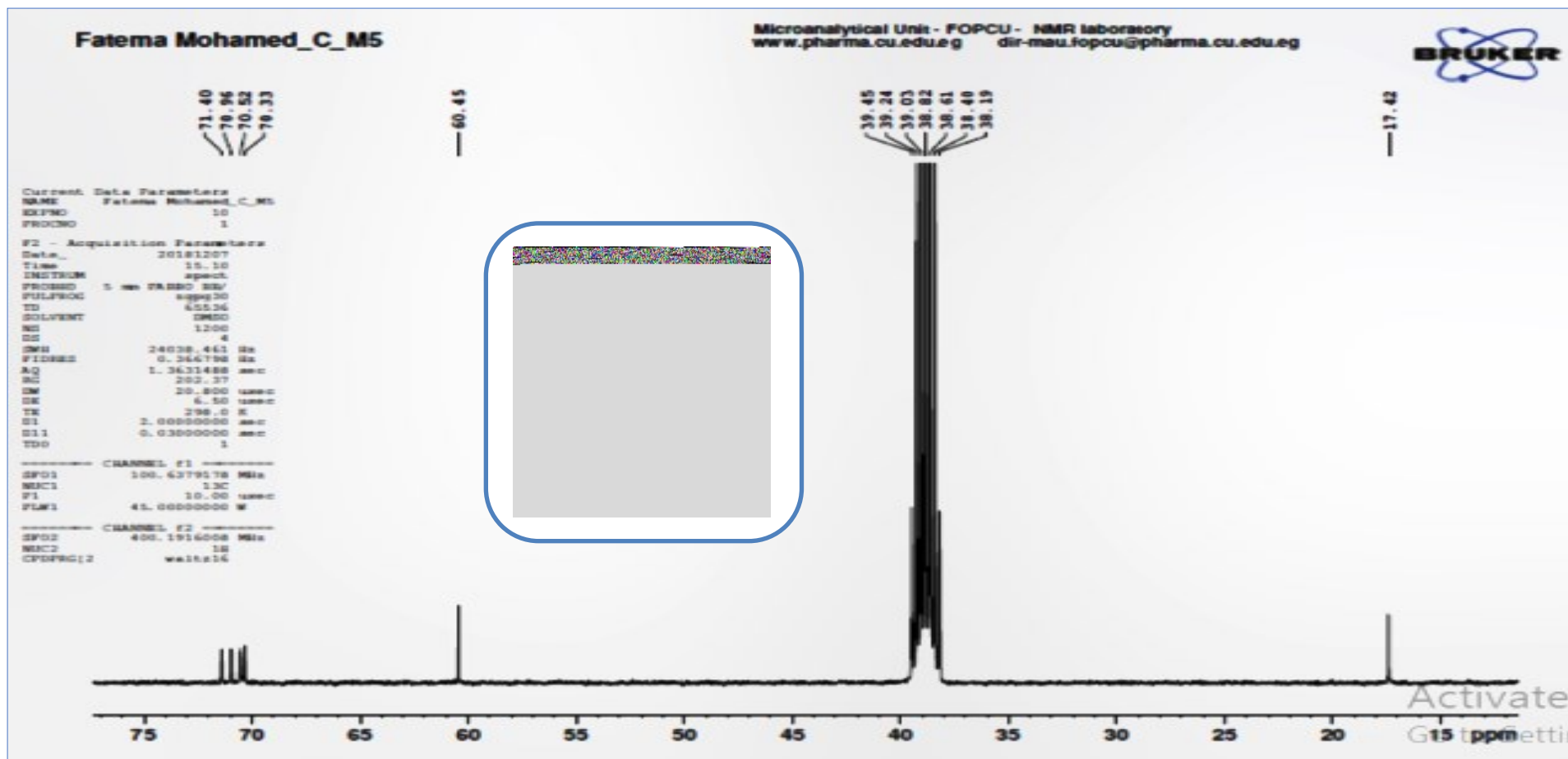


Figure S12: Partial expansion of the ^{13}C -NMR spectrum of compound III in (DMSO- d_6 , 100 MHz)

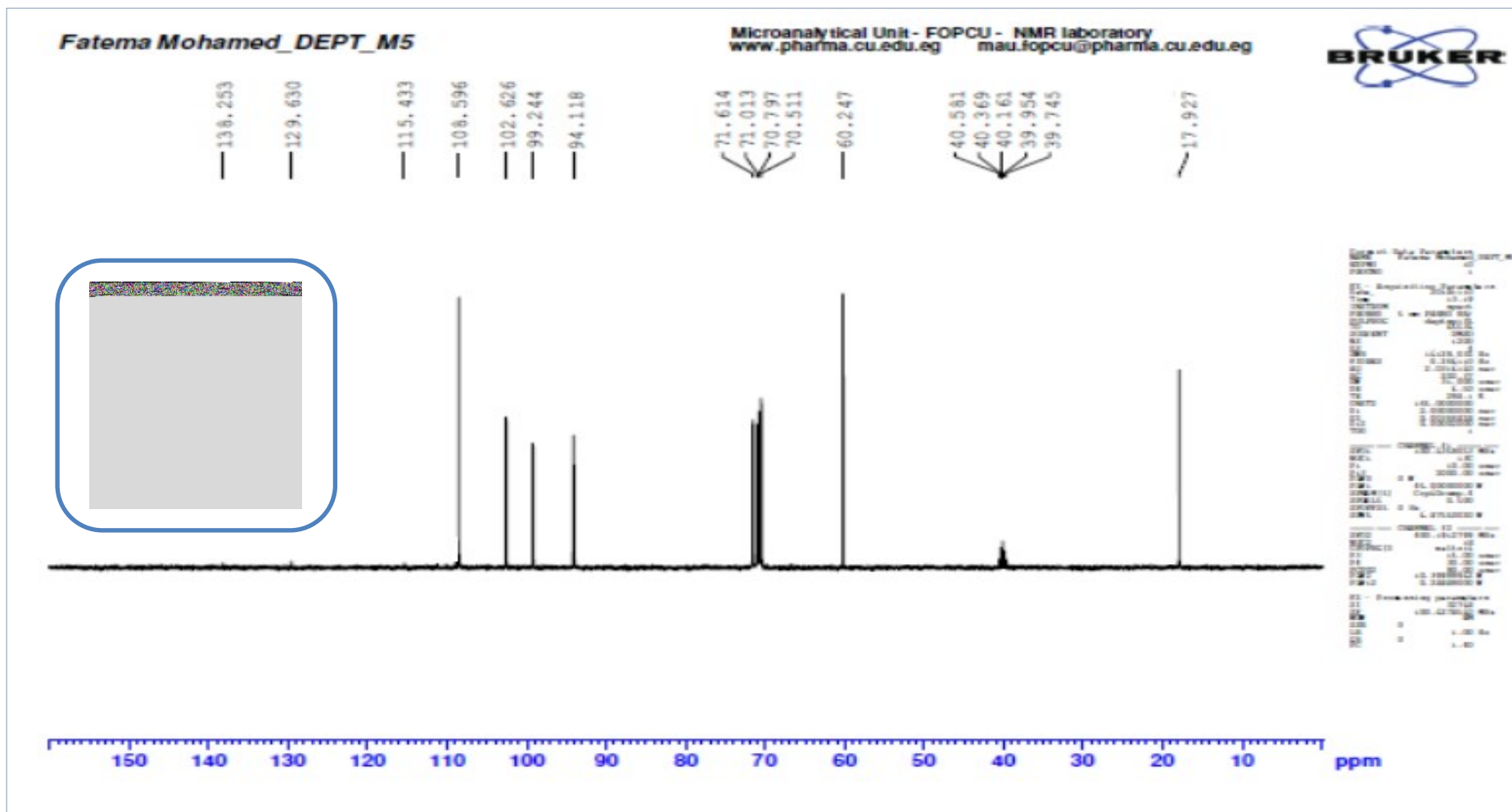


Figure S13: DEPT-135 spectrum of compound **III** in (DMSO- d_6 , 100 MHz)

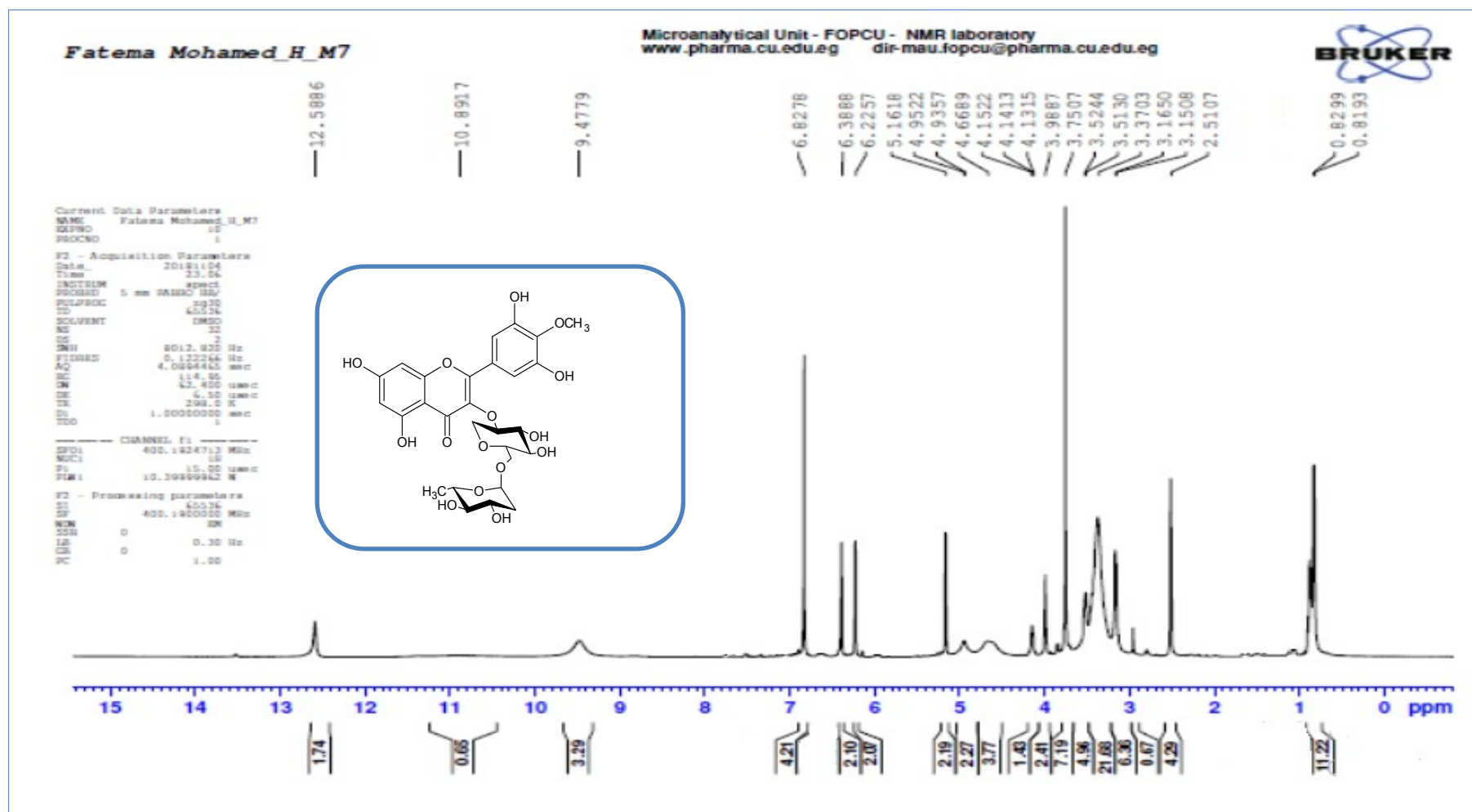


Figure S14: $^1\text{H-NMR}$ spectrum of compound IV in ($\text{DMSO-}d_6$, 400 MHz)

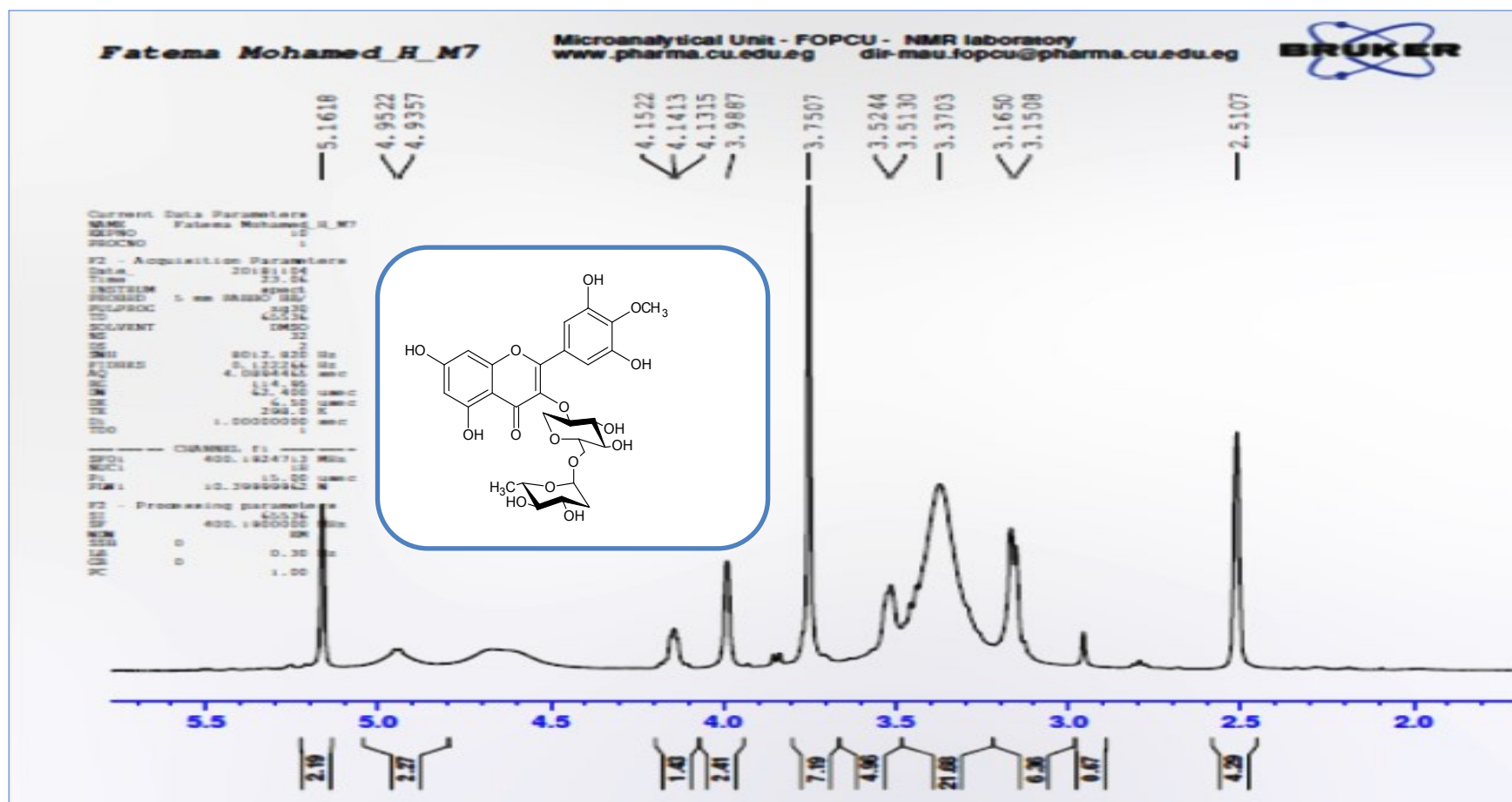


Figure S15: Partial expansion of the ¹H-NMR spectrum of compound IV in (DMSO-*d*₆, 400 MHz)

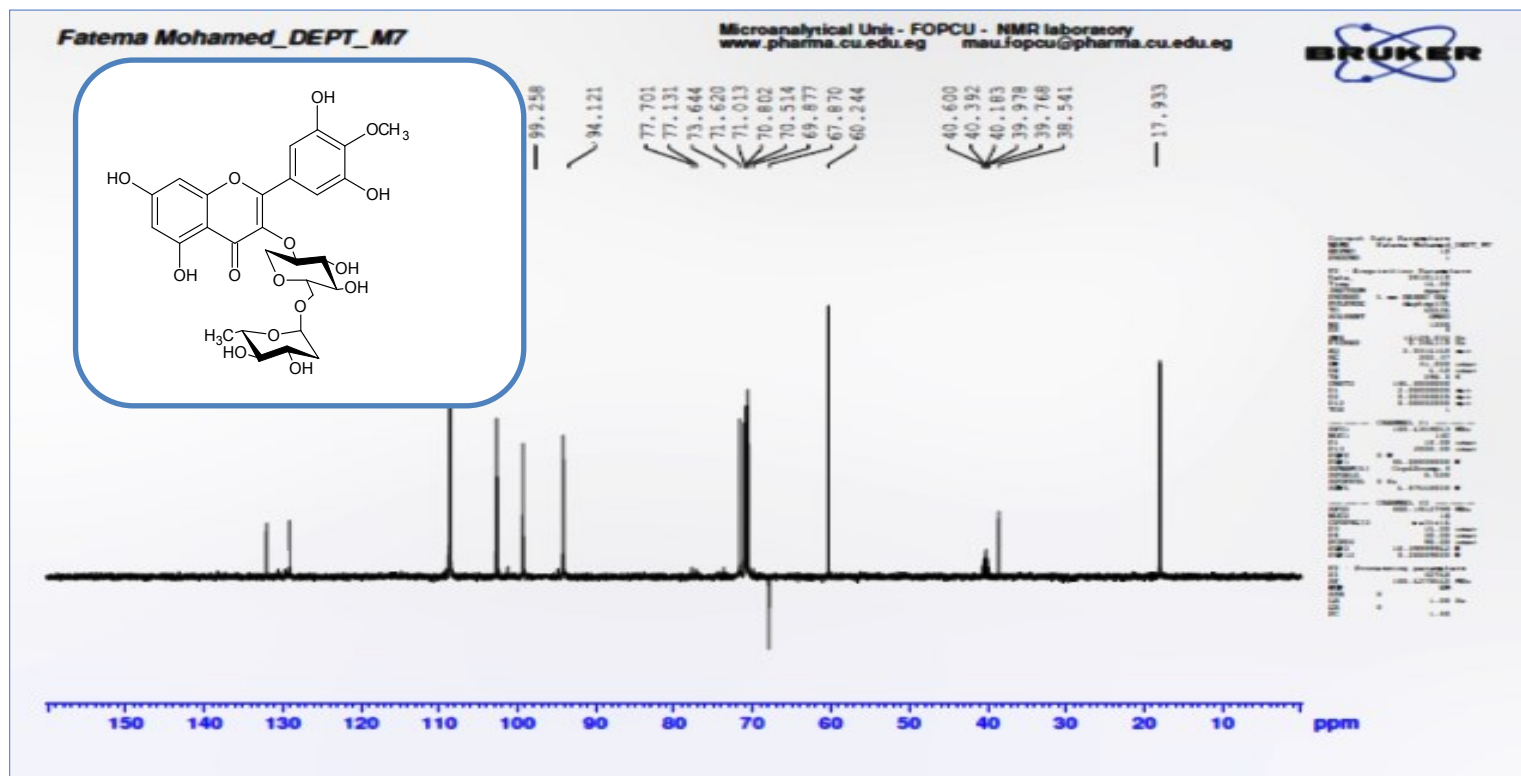


Figure S16: DEPT-135 spectrum of compound IV in (DMSO- d_6 , 100 MHz)

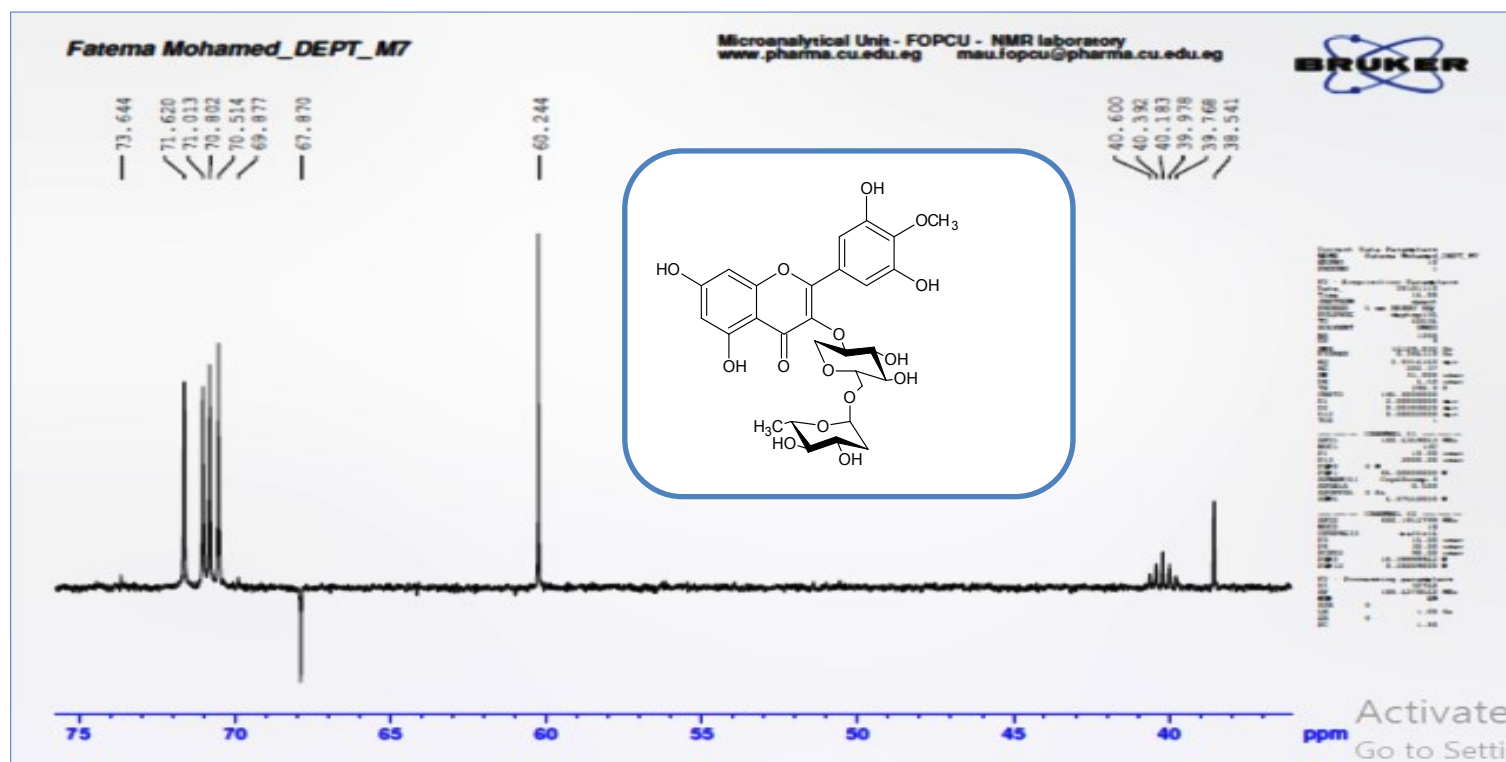


Figure S17: Partial expansion of the DEPT-135 spectrum of compound IV in (DMSO- d_6 , 100 MHz)

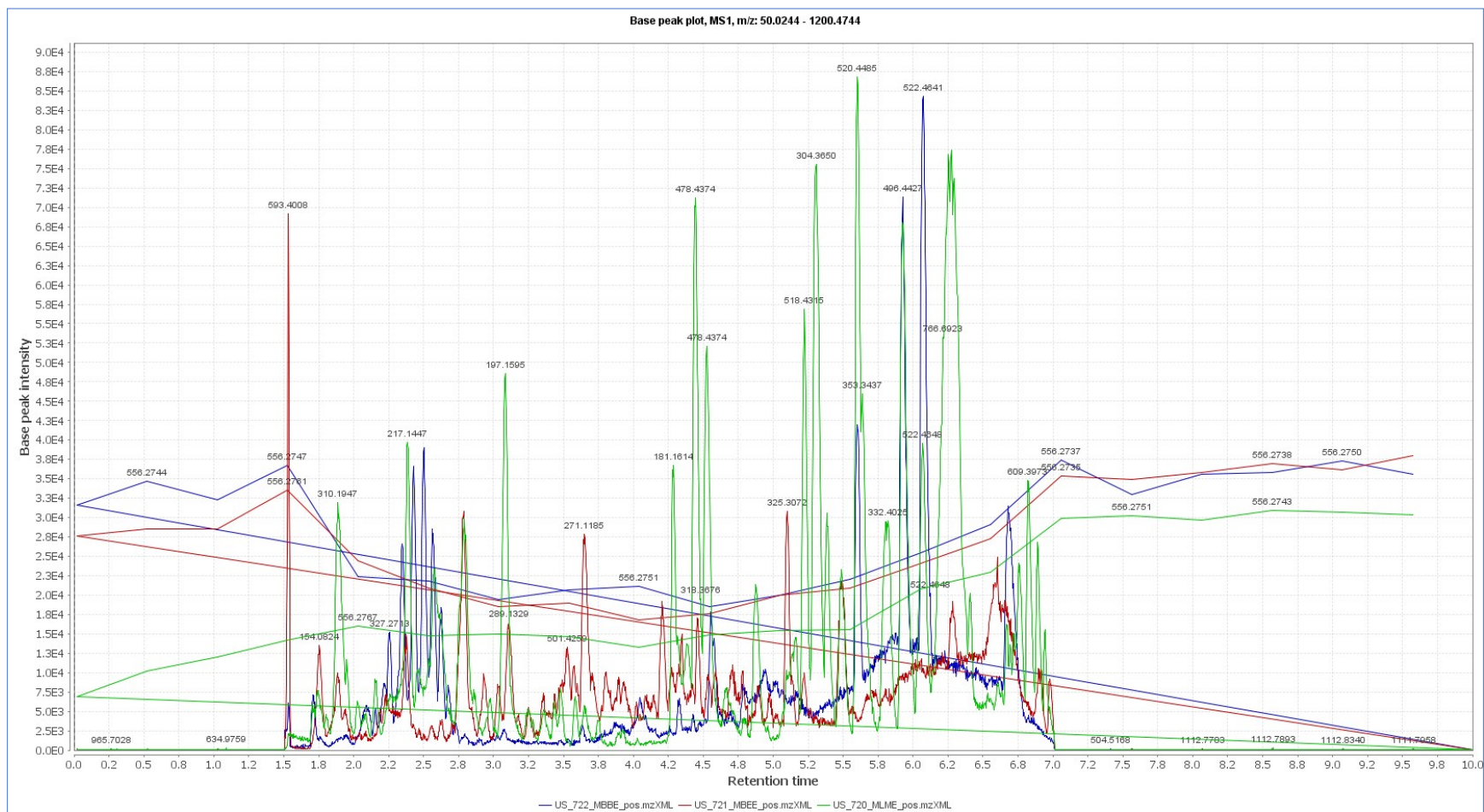


Figure S18: Total Ion chromatogram of different extracts of *Manilkara hexandra* (Roxb.) Dubard.

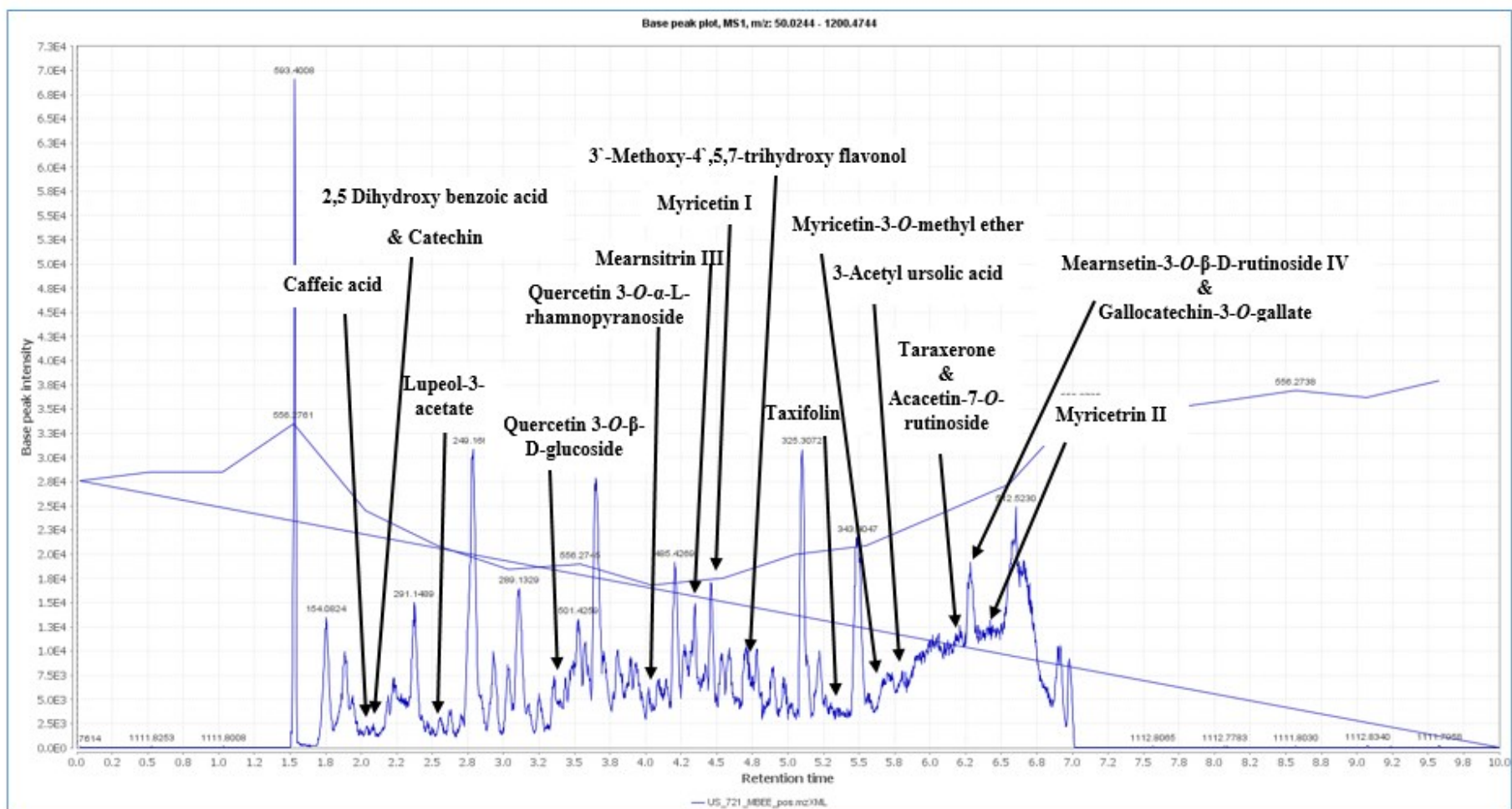


Figure S19: Total ion chromatogram of the ethyl acetate extract of *Manilkara hexandra* (Roxb.) Dubard bark

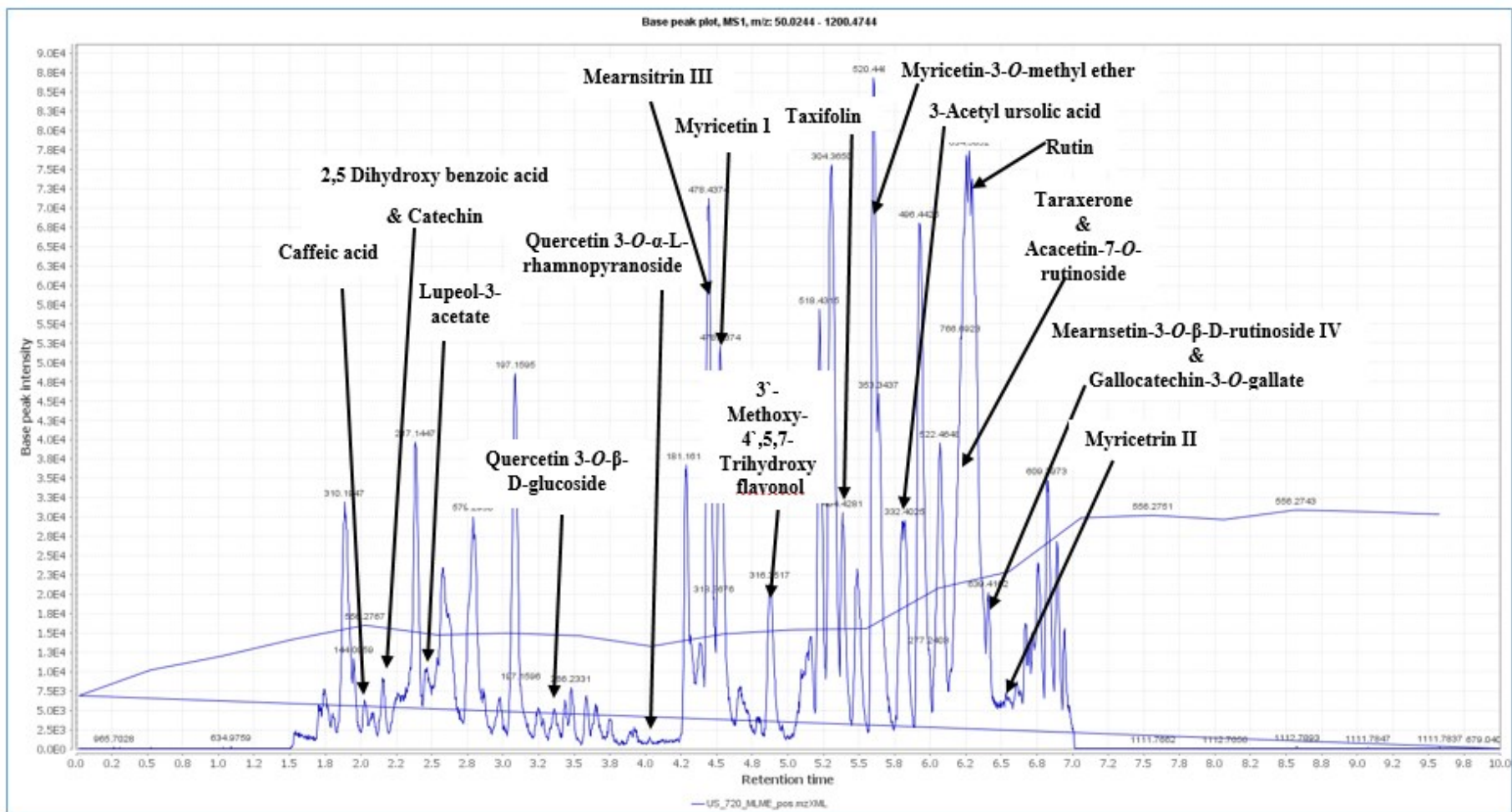


Figure S20: Total ion chromatogram of the methanol extract of *Manilkara hexandra* (Roxb.) Dubard leaves.